Title
Regulated expression of HCN channels and cAMP levels shape the properties of the h current in developing rat hippocampus.

Journal
The European journal of neuroscience, 24(1)

ISSN
0953-816X

Authors
Surges, Rainer
Brewster, Amy L
Bender, Roland A
et al.

Publication Date
2006-07-01

DOI
10.1111/j.1460-9568.2006.04880.x

Published in final edited form as:
Eur J Neurosci. 2006 July ; 24(1): 94–104. doi:10.1111/j.1460-9568.2006.04880.x.

Regulated expression of HCN channels and cAMP levels shape the properties of the h current in developing rat hippocampus

Rainer Surges[1], **Amy L. Brewster**[2], **Roland A. Bender**[2], **Heinz Beck**[3], **Thomas J. Feuerstein**[4], and **Tallie Z. Baram**[2]

[1]Department of Neurology, University Clinics Freiburg, Breisacher Strasse 64, 79106 Freiburg, Germany

[2]Department of Anatomy/Neurobiology, Pediatrics, UCI, Irvine, CA 92697-4475, USA

[3]Department of Epileptology, University of Bonn, Sigmund-Freud Str. 25, 53105 Bonn, Germany

[4]Department of Neurosurgery, University Clinics Freiburg, Breisacher Strasse 64, 79106 Freiburg, Germany

Abstract

The hyperpolarization-activated current (I_h) contributes to intrinsic properties and network responses of neurons. Its biophysical properties depend on the expression profiles of the underlying hyperpolarization-activated, cyclic nucleotide-gated (HCN) channels and the presence of cyclic AMP (cAMP) that potently and differentially modulates I_h conducted by HCN1, HCN2 and/or HCN4. Here, we studied the properties of I_h in hippocampal CA1 pyramidal cells, the developmental evolution of the HCN-subunit isoforms that contribute to this current, and their interplay with age-dependent free cAMP concentrations, using electrophysiological, molecular and biochemical methods. I_h amplitude increased progressively during the first four postnatal weeks, consistent with the observed overall increased expression of HCN channels. Activation kinetics of the current accelerated during this period, consonant with the quantitative reduction of mRNA and protein expression of the slow-kinetics HCN4 isoform and increased levels of HCN1. The sensitivity of I_h to cAMP, and the contribution of the slow component to the overall I_h, decreased with age. These are likely a result of the developmentally regulated transition of the complement of HCN channel isoforms from cAMP sensitive to relatively cAMP insensitive. Thus, although hippocampal cAMP concentrations increased over twofold during the developmental period studied, the coordinated changes in expression of three HCN channel isoforms resulted in reduced effects of this signalling molecule on neuronal h currents.

Keywords

cAMP; development; h current; HCN; hyperpolarization; I_h; ion channel

Introduction

The properties of the hyperpolarization-activated current (I_h) endow it with the capacity to influence excitability of cells and neuronal ensembles (Pape, 1996; Robinson & Siegelbaum, 2003; Santoro & Baram, 2003). This current contributes to regulation of resting membrane potential, input resistance (Surges *et al*., 2004) and synaptic integration (Magee, 1998;

Correspondence: Dr R. Surges, as above. rainer.surges@uniklinik-freiburg.de.

Poolos *et al*., 2002). I_h participates in neuronal activity in thalamocortical networks (Lüthi & McCormick, 1998), and may contribute to network activity in the developing hippocampus (Strata *et al*., 1997; Agmon & Wells, 2003; Bender *et al*., 2005). Age-specific roles for I_h in the maturing rodent hippocampus are supported by developmental expression patterns of hyperpolarization-activated, cyclic nucleotide-gated channel (HCN)1, 2 and 4 genes (Kaupp & Seifert, 2001; Santoro & Baram, 2003). Expression patterns in neonatal rat (Bender *et al*., 2001; Brewster *et al*., 2002) and mouse (Vasilyev & Barish, 2002) differ from those in the mature hippocampus (Moosmang *et al*., 1999; Santoro *et al*., 2000).

The biophysical properties of I_h in native hippocampus only partially overlap those of currents recorded in heterologous systems (Santoro *et al*., 2000; Chen *et al*., 2001; Ulens & Tytgat, 2001; Proenza *et al*., 2002; Xue *et al*., 2002; Much *et al*., 2003). These differences suggest that elements present within native hippocampal neuronal membranes may also influence the properties of the hippocampal I_h. These may include interaction of the neuronal h-channels with putative beta subunits (e.g. minK-related protein-1; Yu *et al*., 2001; Proenza *et al*., 2002; Altomare *et al*., 2003; Qu *et al*., 2004), scaffolding proteins (Gravante *et al*., 2004; Kimura *et al*., 2004) or cytoskeletal proteins (Santoro *et al*., 2004).

During maturation of the hippocampal formation, membrane components of neurons undergo major changes in, for example, neurotransmitter receptors (Simeone *et al*., 2004) and the function of γ-aminobutyric $acid_A$-receptor activation (Rivera *et al*., 1999; Ben-Ari, 2002). These developmental changes and many others may influence the function of neuronal I_h. However, the properties of this conductance are most critically influenced by cyclic AMP (cAMP) that acts directly on the c-terminal intracellular domain of the h channel to rapidly regulate its opening (Wainger *et al*., 2001; see Robinson & Siegelbaum, 2003 for recent review). Importantly, cAMP-mediated gating effects are larger on channels composed of HCN2 and HCN4 compared with those comprised of HCN1 homotetramers, and there is evidence suggesting that cAMP levels in hippocampal neurons may be developmentally regulated (Zhang *et al*., 1999).

Thus, both intracellular cAMP levels and the differential expression of HCN isoforms may govern the properties of I_h in native hippocampal neurons, and both parameters may change during hippocampal development. Here, we studied age-dependent differential expression of HCN channel isoforms, their sensitivity to cAMP and changes in free cAMP concentration as determinants of the properties of I_h recorded from rat CA1 pyramidal cells during the first four postnatal weeks.

Materials and methods

Slice preparation

Hippocampal slices were prepared from 5 to 28 postnatal (P) days old Wistar rats of either sex. Experiments were approved by the Ethical Committee of the Medical Faculty of Freiburg (Germany) and by the UCI animal care committee (IACUC) and followed National Institute of Health (USA) guidelines. Rats were decapitated, the brains were rapidly removed, hemisected and submerged in ice-cold physiological Ringer's solution (Biometra, Göttingen, Germany), which was continuously bubbled with 95% O_2 and 5% CO_2, and contained (in m_M): NaCl, 125; $NaHCO_3$, 25; KCl, 2.5; NaH_2PO_4, 1.25; $MgCl_2$, 1; glucose, 25; $CaCl_2$, 2. The hemispheres were blocked in the horizontal plane and glued to the stage of a vibratome (Leica VT 1000S, Wetzlar, Germany). Horizontal sections through the hippocampus (350–400 μm thick) were cut, and slices were transferred to a holding chamber, where they were submerged in Ringer's solution. This solution was continuously bubbled with 95% O_2 and 5% CO_2 and was maintained at 35 °C for the first 30 min and

then at room temperature (20–22 °C). Slices were kept in the holding chamber for at least 1 h before recordings were performed.

Electrophysiology

Individual slices were transferred into the recording chamber, fixed with a nylon-grid and continuously perfused with oxygenated Ringer's solution at room temperature (20–22 °C). Neurons were then visualized by infrared differential interference contrast video-microscopy with a Newvicon camera (C2400, Hamamatsu, Hamamatsu City, Japan) and an infrared filter (RG9, Schott, Mainz, Germany) to an upright microscope (Axioskop 2 FS, Zeiss, Oberkochen, Germany) equipped with a 40 × water immersion objective. Recordings at room temperature (20–22 °C) were made in the whole-cell configuration of the patch-clamp technique using an Axopatch 200B amplifier and pClamp 8 (Axon Instruments, Foster City, CA, USA). Signals were filtered online at 10 kHz and digitized at 50 kHz during current-clamp experiments, and at 1 kHz and 5 kHz, respectively, during voltage-clamp experiments (Digidata 1200, Axon Instruments). Pipettes were pulled from non-filamented borosilicate glass capillaries (Hilgenberg, Malsfeld, Germany; outer diameter 1.5 mm, inner diameter 1.0 mm) on a P-97 Flaming/Brown horizontal puller (Sutter Instruments, Novato, CA, USA), and had resistances between 3.5 and 5.5 MΩ when filled with the pipette solution. Standard pipette solution contained (in mM): K-gluconate, 130; KCl, 20; $MgCl_2$, 1; $CaCl_2$, 1; HEPES, 10; EGTA, 10; ATP-Tris, 2; GTP-Tris, 0.4; pH 7.25, adjusted with KOH. In a series of experiments, 10 nM, 10 μM or 100 μM cAMP was added to the pipette solution. The offset potential between the patch-pipette and the reference electrode was zeroed before the tight-seal (> 2 GΩ) was established. Cell capacitance, membrane and series resistance were determined by using the 'membrane-test' protocol provided by the software pClamp 8.0. In brief, a test pulse from −63 mV to −53 mV for 15 ms was applied to the cells in the presence of tetrodotoxin (TTX), $NiCl_2$, tetraethylammoniumchloride (TEA), 4-aminopyridine (4-AP) and $BaCl_2$ (see below). By analysing the signal at the end of the test pulse the passive membrane properties were determined. Series resistance was between 8 and 14 MΩ and was monitored during the experiments (compensation up to 60%). The corresponding voltage error was < 3% and therefore neglected. Capacitive transients were not cancelled. Leakage currents were reduced by addition of external Ba^{2+}. Furthermore, a short pulse from −53 mV to −58 mV for 200 ms was applied after each protocol, and the leakage current amplitudes were subtracted offline from the current peaks. A liquid junction potential of +13.0 mV was calculated and all values given are corrected for this voltage offset so that without correction the voltages given in this paper would be 13 mV more positive.

The voltage dependence of I_h activation was examined by measuring tail currents upon relaxation of the serial command potentials to the holding potential (see inset Fig. 3A). The tail current amplitudes were normalized to the maximal tail current amplitude evoked by a command potential of −133 mV and plotted vs. the corresponding precedent command potential. The resulting data points were fit with a Boltzmann equation.

Solutions

The standard bath solution consisted of (in mM): NaCl, 120; $NaHCO_3$, 25; KCl, 2.5; $MgCl_2$, 1; glucose, 25; $CaCl_2$, 2. To isolate I_h during voltage-clamp experiments, the following substances were added (in mm): TTX (Tocris, Biotrend Chemikalien, Köln, Germany), 0.01; $NiCl_2$, 1.0; TEA, 10; 4-AP, 2; $BaCl_2$, 0.5. In a subset of voltage-clamp experiments, 20 μM bicuculline and 10 μM NBQX (Tocris) were added to the bath solution to block spontaneous synaptic events, without significant differences between I_h in the absence and presence of these two substances in P5 and P22 (data not shown). Unless indicated otherwise, drugs were purchased from Sigma (Taufkirchen, Germany).

Analysis

Data were acquired with the help of pCLAMP 8.0 and analysed offline using the software packages Clampfit 8.0 (Axon Instruments) and GraphPad PRISM 2.0 (GraphPad Software, San Diego, CA, USA). In order to determine the time constants of activation and deactivation, the following double exponential term was used with the Chebyshev fitting routine of Clampfit 8.0:

$$f(t)=(A1 \times e^{-t/\tau 1})+(A2 \times e^{-t/\tau 2})+C$$

with A being the current amplitude, τ the time constant and C a constant. The fittings were made from a time point where there was no interference with capacitive transients. Boltzmann fits were made using a least-squares non-linear curve-fitting routine in GraphPad PRISM in order to determine the activation curve with the following equation:

$$I_{tail}/I_{tail,max}=1/\{1+\exp[(V-V_{1/2})/s]\}$$

with $V_{1/2}$ being the midpoint activation voltage and s being the slope. Linear regression analysis to obtain the reversal potential of I_h was also performed with GraphPad PRISM. Statistical significance ($P < 0.05$) was assessed using the two-tailed unpaired or paired Student's *t*-test. All data were expressed as mean ± SEM.

Quantitative *in situ* hybridization (ISH)

For ISH procedures, rats were quickly decapitated at P6, 14 or 25–26 (four rats per group), and brains dissected onto powdered dry ice as described (Brewster *et al*., 2002, 2005). Quantitative analyses of hippocampal HCN isoforms mRNA levels were accomplished using antisense ^{35}S-cRNA probes synthesized by *in vitro* transcription from cDNAs containing specific gene regions of mouse HCN1, HCN2 and HCN4 channels as previously described (Brewster *et al*., 2002; Bender *et al*., 2003). Briefly, 20-μm brain sections were cut, mounted on gel-coated slides and fixed in 4% paraformaldehyde. Following a graded ethanol treatment, sections were exposed to acetic anhydride-triethanolamine, then dehydrated through 70–100% ethanol. Sections were then preincubated in hybridization solution [50% formamide, 5 × sodium EDTA-Tris (SET), 0.2% sodium dodecyl sulphate (SDS), 5 × Denhardt's solution, 0.5 mg/mL salmon sperm sheared DNA, 250 μg/μL yeast tRNA, 100 mM dithiothreitol, 10% dextran sulphate] and probed overnight at 55 °C with antisense ^{35}S-CTP-radiolabelled HCN probes (0.5–1 × 10^6 cpm/30 μL/section). The specific activities of the probes were 0.48–5.4 × 10^9 cpm/μg. On the following day, sections were washed in decreasing concentrations of saline sodium citrate (SSC) solutions, with the most stringent wash at 0.03 × SSC for 60 min at 62 °C. Following dehydration in increasing alcohol concentrations, sections were apposed to Kodak Biomax films. Optimal exposure time was monitored using ^{14}C standards to maintain signal linearity.

Western blot (WB) procedures

For protein analyses, each sample consisted of a hippocampal-CA1 extract from an individual rat. For Western blot analyses, rats of different ages (P6, P14 or P26; four–six rats per group) were rapidly decapitated and hippocampi quickly dissected, area CA1 isolated, and tissue frozen immediately in powdered dry ice. CA1 tissue blocks from individual animals were homogenized in glass/Teflon homogenizers in ice cold 0.32 M sucrose, 0.1 M Tris–HCl (pH 7.4) Protease Inhibitor Cocktail according to the manufacturer's instructions (PIC Complete™; Roche, Indianapolis, IN, USA). Samples were then centrifuged at 1000 ***g*** for 10 min at 4 °C and pellet discarded. The resulting supernatant was centrifuged at 16 000

g for 20 min at 4 °C and the pellet containing membrane fractions was resuspended in artificial cerebrospinal fluid (in m_M: NaCl, 124; KCl, 3; KH_2PO_4, 1.25; $MgSO_4$, 2.5; $CaCl_2$, 3.4; $NaHCO_3$, 26; glucose, 10; 1 × PIC). Protein concentration was determined using Bio-Rad protein assay (Bio-Rad Laboratories, Hercules, CA, USA). Equal amounts of protein were diluted in Laemmli buffer, separated by SDS–polyacrylamide gel electrophoresis (PAGE) and visualized using the enhanced chemiluminescence ECL-Plus kit (Amersham Pharmacia Biotech; Piscataway, NJ, USA) as previously described (Brewster *et al*., 2005). Briefly, 20 μg of protein extracts was separated on a 4–12% SDS–PAGE and transferred to Hybond-P polyvinyldifluoride membranes (Amersham Pharmacia Biotech). Membranes were blocked with 5% non-fat milk in 1 × phosphate-buffered saline (PBS) overnight, and probed overnight (at 4 °C) with rabbit anti-HCN1 (1 : 500; Chemicon, Temecula, CA, USA) or rabbit anti-HCN2 serum (Alomone, Jerusalem, Israel; lot #AN-06; 1 : 500 dilution in 1 × PBS−2.5% milk). The authors note that different antisera for HCN2 may have somewhat differing selectivities, and may recognize different species of this molecule. For HCN4 detection, membranes were probed with guinea pig anti-HCN4 (1 : 500) for 1 h at room temperature as described in Notomi & Shigemoto (2004). Protein content was normalized using actin, detected using rabbit anti-actin (1 : 40 000; Sigma) as an internal and loading standard. Following washes in PBS−1% Tween (PBS-T) (three times, 5 min each), membranes were probed with secondary antibodies (donkey anti-rabbit IgG or rabbit anti-guinea pig IgG conjugated to horseradish peroxidase 1 : 10 000; Amersham Pharmacia Biotech or Sigma, respectively) in PBS-T for 1 h at room temperature. Membranes were then washed in PBS-T (three times, 5 min each) and incubated with ECL-Plus. Immunoreactive bands were visualized by apposing membranes to Hyperfilm TM ECL (Amersham Pharmacia Biotech). CA1 extracts of individual rats of different age groups were run concurrently on the same gel.

HCN channel data quantification and analyses

All quantitative analyses were performed by investigators unaware of the age group of the samples. Data acquisition and quantification of *in situ* hybridization signals were carried out as described elsewhere (Brewster *et al*., 2002; Bender *et al*., 2003) on sections run concurrently. Quantification and statistical analyses of HCN mRNA signal were accomplished by measuring optical density of incorporated radioactivity in CA1 using the image analysis program ImageTool (version 1.25; University of Texas Health Science Center, San Antonio, TX, USA). Optical density measured over the corpus callosum was used as a background signal and subtracted from the signal measured over the CA1 pyramidal cell layer. Linearity of the hybridization signal was ascertained using ^{14}C standards (American Radiolabelled Chemicals, St. Louis, MO, USA). WB data acquisition and analysis were accomplished by measuring optical density of the HCN1, HCN2 or HCN4 immunoreactive bands as described (Brewster *et al*., 2006); the signal was then normalized to the actin content of each individual sample (Brewster *et al*., 2005). In addition, actin content served as a reference for determining the relative abundance of each HCN channel isoform in samples probed with different antisera. Statistical analyses for ISH and WB data were performed using GraphPad Prism software (GraphPad Software, San Diego, CA, USA). Significance level (set at $P < 0.05$) was determined using one-factor ANOVA followed by Bonferroni's *post hoc* test. Data are presented as means with standard errors.

cAMP measurements

Hippocampal cAMP concentration was determined using a commercial radioimmunoassay kit utilizing cAMP labelled with ^{125}I (Direct Biotrak Scintillation Proximity Assay System; Amersham Pharmacia Biotech) according to manufacturer's instructions. Each sample consisted of a hippocampal extract from an individual rat. Rats aged 6, 16 or 23 days ($n = 4$/age group) were decapitated and hippocampi dissected rapidly onto powdered dry ice (note

that pilot time course experiments excluded cAMP degradation under these conditions). Frozen samples were weighed, then homogenized in glass homogenizers in ice cold 6% (w/v) trichloroacetic acid (TCA) at 2–8 °C. Hippocampal samples were centrifuged at 2000 ***g*** for 15 min at 4 °C and pellets used for determining protein concentration using the Bradford Assay (Bio-Rad, Hercules, CA, USA). The supernatant was washed 4 × with 5 volumes of saturated diethyl ether to remove TCA. The aqueous extract was lyophilized and cAMP concentration assayed using the kit above, according to the manufacturer's instructions. Statistical analyses of cAMP measurements were performed using ANOVA followed by Bonferroni's *post hoc* test.

Results

Basic properties of I_h in CA1 neurons of developing hippocampus

The present study includes information from 108 visually selected cells within the pyramidal cell layer of CA1. At the onset of each experiment, a family of current pulses was applied to each cell in the current-clamp mode. As expected for maturing neurons, R_M decreased from 450 ± 30 MΩ in P5–7 neurons (n = 44) to 170 ± 6 MΩ in neurons from rats aged P22–28 (n = 33, $P < 0.001$), whereas C_M substantially increased from 75 ± 3 pF (n = 44) to 168 ± 8 pF, indicative of an increase in cell surface (n = 33, $P < 0.001$, Fig. 1B, representative voltage traces of cells from P6 and P25 in Fig. 1A). Prolonged depolarizing current injection evoked a train of action potentials displaying spike adaptation, a behaviour typical for CA1 pyramidal neurons (e.g. Costa *et al*., 1991;Azouz *et al*., 1997). Therefore, only cells in which this adaptation occurred were included in this study. It should be noted that we did not observe cells that fired in a bursting mode, even though a transitional period of bursting has been described for CA1 neurons peaking at about P18 (Costa *et al*., 1991;Chen *et al*., 2005). This is most likely due to the fact that we employed patch-clamp recordings, in which the propensity to burst may be lower than in sharp microelectrode recordings (cf. Chen *et al*., 2005 vs. Costa *et al*., 1991). In addition, some of these differences may have arisen because of different intra- and/or extracellular solutions that also affect bursting. In all cells, we found a 'voltage sag' upon hyperpolarizing current injection, indicative of the presence of I_h (see asterisk in Fig. 1A).

Currents mediated by I_h were then recorded in voltage-clamp mode by applying hyperpolarizing voltage steps. The amplitude of I_h was determined by subtracting the instantaneous current at the beginning of the voltage step from the steady-state current at the end (Fig. 1C). The amplitude of I_h increased steeply as a function of postnatal age, from −124 ± 25 pA at P5 to −334 ± 12 pA at P28 (Fig. 1D). In order to obtain current–voltage relationships, the averaged I_h amplitudes of neurons from P5–7 and P22–28 were plotted vs. the command potential. As shown in Fig. 1E, the amplitude of I_h increased with increasing amplitude of the command potential, and the current amplitudes in the P22–28 group (n = 21) were significantly higher than in P5–7 (n = 20) within the voltage range tested ($P < 0.0001$). Because the surface of CA1 pyramidal cells increases during brain maturation, we sought to estimate the current density of I_h. To this end, we divided I_h amplitudes by the cell capacitance (Fig. 1B), which constitutes a rough approximation of the cell area. The current density proved to be similar in cells from P5–7 (−2.4 ± 0.2 pA/pF, n = 20) compared with cells from P22–28 (−2.1 ± 0.1 pA/pF, n = 20, n.s.).

To test whether age-related changes in the driving force occur during postnatal development that may influence the current amplitudes, we determined the reversal potential using conventional methods (see Surges *et al*., 2002 for detailed procedure). The reversal potential was unaltered in animals aged P5–7 (−39.3 ± 5.4 mV, n = 9) and P22–28 (−39.0 ± 5.22 mV, n = 7, not shown).

Functional properties of I_h change dramatically during development

Because different HCN subunits possess characteristic time courses of activation and deactivation, we examined age-related changes in I_h kinetics. The time course of I_h activation was best described as the sum of two exponential equations throughout the age range investigated. The representative current traces depicted in Fig. 2A already suggest that the time course of I_h activation is accelerated in older age groups. A quantitative analysis of I_h activation revealed that both the fast and slow time constant describing the biexponential activation time course, $\tau_{fast,act}$and $\tau_{slow,act}$, decreased during development (Fig. 2B). Because the activation time course is voltage dependent in adult mice (Santoro *et al*., 2000), we studied the voltage dependence of $\tau_{fast,act}$ and $\tau_{slow,act}$ in two age groups (P5–7 and P22–28, Fig. 2C). As expected, both $\tau_{fast,act}$ and $\tau_{slow,act}$ were voltage dependent in developing hippocampal CA1 neurons, with faster activation at more hyperpolarized command potentials (Fig. 2C). Within a voltage range of −113 to −133 mV, $\tau_{fast,act}$ was significantly shorter in the older age group (at −133 mV: 111 ± 14 ms, n = 20 at P5–7 compared with 60 ± 2 ms, n = 21 at P22–28, P = 0.0008, see Fig. 2C left panel). Similar findings were obtained for $\tau_{slow,act}$ (at −133 mV: 695 ± 44 ms at P5–7 compared with 513 ± 25 ms at P22–28, P = 0.0007, see Fig. 2C right panel).

The activation time course of I_h is not exclusively determined by the two rate constants $\tau_{fast,act}$ and $\tau_{slow,act}$. Rather, the relative contribution of the fast vs. the slow time constant to the activation kinetics may also play a large role. Therefore, we derived these relative amplitudes from our biexponential fitting paradigms (Fig. 2D). In neurons from P5–7 rats, the contribution of the fast-activating component was significantly lower as compared with cells from P22–28 rats (Fig. 2D, $P < 0.001$ indicated by asterisks). Interestingly, this parameter was voltage dependent in P5–7 rats (Fig. 2D; amplitude contribution of 0.36 ± 0.05 at −113 mV and 0.56 ± 0.03 at −133 mV, paired t-test $P < 0.0001$, n = 20), but not in P22–28 animals (0.77 ± 0.02 at −113 mV and 0.76 ± 0.02 at −133 mV, n = 21).

To evaluate the time course of I_h deactivation, the tail current trace evoked by a preceding test pulse to −133 mV for 2 s, relaxing to the holding potential of −63 mV, was fit with the sum of two exponential equations. The value of $\tau_{fast,deact}$ was lower in P22–28 (146 ± 7 ms, n = 21) as compared with P5–7 (P = 0.045, 192 ± 23 ms, n = 20), whereas $\tau_{slow,deact}$ was not significantly affected during development (523 ± 49 ms in rats from P5–7 and 468 ± 79 ms in rats from P22–28; P = 0.56, not shown).

The voltage dependence of I_h activation was then analysed as described in the Materials and methods. To investigate the cAMP-naïve HCN subunits and to exclude possible differential effects of cAMP, these initial experiments were conducted without cAMP in the intracellular solution. A comparison between the activation curve of CA1 pyramidal cells from P5–7 and P22–28 rats revealed a significant shift of $V_{1/2}$ to more depolarized potentials, from −102.2 ± 0.6 mV (n = 20) to −91.6 ± 0.7 mV in P22–28 neurons ($P < 0.001$, n = 21; Fig. 3A). The slope factor s was not changed during postnatal development (−10.4 ± 0.5 mV at P5–7 and −10.5 ± 0.7 mV at P22–28). An analysis of $V_{1/2}$ over a range of postnatal ages revealed a progressive shift that appeared to be most pronounced between P11 and P14 (Fig. 3B). The large shift of $V_{1/2}$ raised the question whether the faster kinetics observed in older animals might be caused in part by the altered voltage dependence of I_h. To better estimate the contribution of $V_{1/2}$ changes to the time course, the respective values of each age group were compared at command potentials that are close to $V_{1/2}$: the values for I_h amplitude and current kinetics at −103 mV for P5–7 neurons and at −93 mV for P22–28 neurons, respectively (Fig. 3C). The differences in the fast activation time constants were still statistically significant, indicating that the shift in $V_{1/2}$ alone cannot explain the age-dependent alterations of these parameters.

Voltage-related I_h activation is strongly modulated by intracellular cAMP (Pape, 1996; Kaupp & Seifert, 2001; Wainger *et al*., 2001; Robinson & Siegelbaum, 2003). In the results described so far, the recordings were carried out with intracellular solutions lacking cAMP. In the following paragraph, we discuss studies investigating whether the sensitivity to the modulatory effects of cAMP varied with age. To this end, we compared recordings in which the pipette solution contained 10 μM internal cAMP to recordings without cAMP. Voltage-clamp experiments were started 10–15 min after obtaining the whole-cell configuration to promote equilibration of the internal milieu (but see Budde *et al*., 2005). The presence of cAMP caused a change in $V_{1/2}$ only in neurons from the younger age group (from −102.2 ± 0.6 to −97.7 ± 1.0 mV, $n = 7$, $P < 0.001$, Fig. 3D and inset). In cells from animals aged P22–28, $V_{1/2}$ was unchanged by the addition of cAMP ($V_{1/2}$ in the presence of 10 μM cAMP: −91.8 ± 0.9 mV, $n = 7$, Fig. 3D and inset). The slope factor *s* remained unchanged at either age. These data indicate that h channels from P5–7 neurons are intrinsically more responsive to the effects of cAMP. Indeed, cAMP sensitivity of $V_{1/2}$ in P5–7 neurons was exquisite: when tested at internal cAMP concentrations of 10 nM and 100 μM, robust effects occurred already at a concentration of 10 nM, and the effect of 10 μM cAMP on $V_{1/2}$ was essentially saturating (Fig. 3E). These results also indicate that we have essentially clamped the cAMP concentration in the intracellular milieu to values governed by the pipette solution with little contamination by endogenous cAMP.

This remarkable, age-specific sensitivity of h channels of P5–7 neurons to cAMP prompted questions about its molecular basis. Interestingly, h channel-opening enhancement upon prolonged hyperpolarization in the presence of low concentrations of cAMP has recently been shown, and is considered to occur via allosteric coupling (Wang *et al*., 2002). This altered open state of the channel may produce long-lasting changes in its function. To consider this possibility, we applied relatively long (5 s) pulses to P5–7 neurons in the absence and presence of cAMP, and tested both a low concentration (10 nM) as well as a high one (100 μM). The resulting current traces were fit with both a two-exponential as well as a three-exponential equation, the latter designed to uncover potential additional slow current component as an indicator of the allosteric transition of I_h channels. At −123 mV, only the current traces in the presence of 10 nM cAMP were significantly better fit with a three-exponential equation (goodness of fit expressed as sum of squared errors: two-exponential equation: 435 600 ± 78 270; three-exponential equation: 426 000 ± 78 800; $n = 6$; $P < 0.01$, paired *t*-test, data not shown). The corresponding time constants resulting from a three-exponential fit yielded a fast (110 ± 9 ms), a slow (493 ± 110 ms) and an additional ‘ultra-slow’ time constant (3515 ± 1324 ms). At −123 mV, this putative ultra-slow current component contributed 25 ± 3% to the total current amplitude, whereas the fast current component made up 48 ± 2%. The potential function and physiological significance of this putative ultra-slow component of I_h in developing hippocampus are unclear.

Taken together, the findings described above show that the properties of I_h in hippocampal CA1 pyramidal cells change dramatically during the first four postnatal weeks. This conductance evolves from a slow- to a fast-gating phenotype, and the voltage-dependent activation as well as the sensitivity to cAMP-modulation is altered.

Quantitative developmental changes in the expression of HCN channel isoforms may contribute to the age-specific properties of I_h in CA1 pyramidal cells

The shift in the voltage dependence of I_h activation in the depolarized direction with age, as well as the significant acceleration of the channel’s kinetics, prompted analysis of the molecular basis of I_h throughout the first few postnatal weeks. The changes in cAMP gating further promoted this analysis, because they are largely dependent on the HCN isoform composition of the channels, and are more pronounced in channels comprised of HCN4 and HCN2 (compared with HCN1). Of the four characterized members of the HCN channel

gene family, three: HCN1, 2 and 4; were significantly expressed in hippocampal CA1 neurons of the developing rat (Fig. 4A–C, photomicrographs). Quantitative analyses of the mRNA levels of these channels revealed substantial isoform- and age-dependent changes in their expression (Fig. 4). Consistent with the accelerated kinetics of the I_h recorded from CA1 neurons, the mRNA expression of the fast-kinetics HCN channel isoform, HCN1, increased progressively as a function of age (1.7-fold between P6 and P26: $F_{2,8} = 14.3$, $P < 0.01$; Fig. 4A). Note that this increase was also evident when expressed per unit of hippocampal protein (Fig. 4A). In contrast, a strong reduction in the expression of the HCN channel isoform with the slowest kinetics, HCN4, occurred during the same period (P6–26: $F_{2,9} = 33.8$, $P < 0.0001$; Fig. 4C). Expression levels of HCN4 mRNA in CA1 pyramidal cell layer on P26 were only 56 ± 2.8% of levels at P6 (Fig. 4C; $P < 0.001$). The age-dependent expression profile of HCN2 resembled neither HCN1 nor HCN4 (Fig. 4B), demonstrating some increase between P6 and P14, with little further variation with age (P6–26: $F_{2,9} = 1.2$, $P > 0.05$). The relative contribution of the HCN1, 2 and 4 mRNA levels to the total HCN mRNA pool as a function of age is shown in Fig. 4D, highlighting the reciprocal transcriptional regulation of HCN1 and HCN4 during the first four postnatal weeks.

Protein expression of the HCN channel isoforms was generally concordant with the mRNA levels (Brewster *et al*., 2005, 2006): HCN1 protein levels in hippocampal CA1 (expressed per actin levels of the same sample) increased almost threefold between P6 and P26, from 79 ± 6.4 to 210 ± 21 OD/actin; $P < 0.0001$; Fig. 5A. In contrast, HCN4 protein expression during the fourth postnatal week dropped to 18% of the P6 levels, from 76 ± 7.3 to 14 ± 2.1 OD/actin ($P < 0.001$; Fig. 5C). In general agreement with the mRNA levels, protein expression of the HCN2 isoform was 48 ± 8.6 OD/actin on P6, 91 ± 4.5 on P14 and 95 ± 6.6 OD/actin on P26 (Fig. 5B). Thus, the protein levels also demonstrated the highly divergent developmental expression patterns of the three HCN channel isoforms. Estimates about the relative contributions of HCN1, HCN2 and HCN4 to the total h channel complement of CA1 pyramidal cells as a function of age are schematized in Fig. 5D. The graph suggests that HCN1 should contribute only 38% of the current at P6, and close to 2/3 of the I_h (65%) on P26. In contrast, the corresponding values for HCN4 are 37% at P6 and only 4.3% at P26. Importantly, this developmental ‘switch’ of the contribution of HCN1 and HCN4 to I_h recorded from CA1 pyramidal cells governs also the strikingly reduced sensitivity of this conductance to cAMP.

Developmental changes in cellular cAMP concentrations may further modulate HCN channel function

As shown above, cAMP potently modulates I_h in CA1 pyramidal cells of developing hippocampus, via shifting the voltage-dependent activation curve and also by contributing to the emergence of a very slow component of I_h activation during long hyperpolarizing pulses (potentially indicating allosteric modulation). The molecular basis for a reduction of cAMP effects on I_h in older neurons may be attributable to the ‘shift’ in the relative abundance of HCN channel isoforms during this period, from high contribution (64%) of the cAMP-sensitive HCN4/HCN2 isoforms during the first postnatal week to an increased contribution of the relatively cAMP-insensitive HCN1 and reduced percent abundance of HCN2/4 (34%) during the fourth postnatal week (Figs 4D and 5D). This striking reduction in cAMP sensitivity raised the question of the potential functional relevance of this developmental change. Is the molecular switch of HCN subunits expression associated with (or perhaps a countermeasure for) a coordinated regulation of cAMP during maturation? We therefore examined quantitatively cAMP levels in the hippocampus and found that cAMP concentrations vary significantly with age, increasing robustly during development ($F_{2,11} = 35.4$, $P < 0.0001$; Fig. 3E): levels of this nucleotide more than doubled between P6 and P15 (from 54 ± 6.3 to 128 ± 2.6 fmol/μg protein; $P < 0.001$), and remained at the higher level

during the fourth postnatal week. These data suggest that functional changes in I_h during development are likely influenced by simultaneous changes of the molecular properties of the channel as well as changes in cAMP concentration.

Discussion

The principal findings of these studies are as follows. (1) I_h amplitude increases progressively during the first four postnatal weeks, consistent with overall increased expression of the HCN isoforms. (2) The kinetics of the current accelerate, including both fast and slow components, in accordance with a reduced expression of the slow-kinetics HCN4 isoform and increased levels of HCN1 mRNA. (3) The sensitivity to modulation by cAMP decreases with age, likely attributable to simultaneous increased HCN1 and reduced HCN4 isoform expression. (4) These changes occur concurrently with progressively increasing levels of hippocampal cAMP concentrations, and may 'protect' neurons from cAMP-evoked, I_h hyperexcitability.

Progressive upregulation of I_h during development

The progressive increase of the I_h amplitude is consistent with previous work in the mouse (Vasilyev & Barish, 2002). The I_h in hippocampal CA1 is conducted via channels formed by the HCN1, HCN2 and HCN4 isoforms, in homomeric (Moosmang *et al*., 1999; Franz *et al*., 2000; Santoro *et al*., 2000; Bender *et al*., 2001; Brewster *et al*., 2002) and perhaps heteromeric configurations (Brewster *et al*., 2005). Concomitant with the ~200% increase of I_h amplitude during development, expression of HCN1 mRNA increased by 60%, that of HCN2 increased modestly, and HCN4 mRNA levels decreased by 44%. Whereas the relationship between mRNA and protein expression may not be linear, because it is governed by mRNA turnover, translation efficiency, protein turnover and many other factors, HCN1 mRNA and protein levels in developing rat hippocampus have generally been found to be concordant (Brewster *et al*., 2002, 2005). Indeed, in the present study, HCN1 protein levels in CA1 increased by ~170% between the first and fourth postnatal weeks, HCN2 protein increased by 78% and protein expression of HCN4 declined by ~80%. Given that HCN1-encoded channels may carry more than half of the I_h at this latter age (Fig. 5D), these values are consonant with the observed augmentation of the current's amplitude.

Altered kinetics of I_h during development

A progressively increasing contribution of HCN1 to the macroscopic I_h in CA1 is supported also by the acceleration of activation kinetics of the current as a function of age found here (see also Vasilyev & Barish, 2002), and the described correlation between HCN1 mRNA expression and fast-gating kinetics (Franz *et al*., 2000). Our quantitative molecular data provide an attractive explanation for these differences in biophysical I_h properties. Among the three HCN isoforms that contribute to I_h of CA1, HCN4 channels possess the slowest kinetics ($\tau_{fast,act}$ = 384 ms and $\tau_{slow,act}$ = 2275 ms at −110 mV and 35 °C; Ishii *et al*., 1999). In heterologous systems, the activation and deactivation kinetics of 'pure' HCN1 channels are ~70 ms at −105 mV for activation and ~300 ms for deactivation, approximating the current recorded here (Chen *et al*., 2001). Given the upregulation of HCN1 channels and the concomitant downregulation of HCN4 channels during development, we can estimate that the contribution of HCN1 subunits to I_h channels increases from 39% to 65%. This increased contribution of HCN1 would be expected to result in faster-gating macroscopic I_h. It should be noted that in addition to faster kinetics, I_h from progressively older hippocampus evolved also in their voltage-dependent activation: $V_{1/2}$ shifted ~10 mV in the depolarizing direction, a shift that is also in good agreement with an increased contribution of the HCN1 isoform to the total current (Chen *et al*., 2001). It should be noted that in somatic patch-clamp recordings, as those performed in the present study, distal dendritic

segments are not adequately voltage-clamped. Changes in I_h kinetics during development could therefore also arise via an age-dependent redistribution of HCN subunits during development. We believe that this is unlikely because the subcellular transport to the dendrites of a key molecule conducting this current, HCN1, is already established on P2, when the channels are already concentrated in distal dendrites in the stratum lacunosum moleculare (Brewster *et al*., 2006). Alternatively, it could be that the increase in spatial extent and altered cable properties of the dendrites could cause altered dendritic filtering at early vs. late developmental stages. However, increased dendritic filtering would be unlikely to account for the increasingly faster gating during development.

Effects of cAMP on I_h during maturation

Between the first and fourth postnatal week, fundamental changes occur in both cAMP sensitivity of I_h, and in cAMP concentration. I_h in the younger age group is powerfully modulated by intracellular cAMP, while this is not the case in animals older than 3 weeks. Intriguingly, the cAMP sensitivity of I_h at early postnatal stages is exquisite, because 10 nM cAMP already causes pronounced effects on I_h voltage dependence.

Thus, our results establish that the I_h of CA1 pyramidal cells is potently modulated by cAMP early in postnatal life, but not at older ages. Over the same period, cAMP levels in the hippocampus increase quite radically. What purpose would this striking reduction of cAMP sensitivity of I_h serve? An attractive explanation suggests that intraneuronal cAMP-dependent signalling is highly upregulated during postnatal development, and serves many cellular purposes. Because cAMP is not only an intracellular signalling molecule, but also binds to and modulates ion channels such as I_h, it may become necessary to generate cAMP-insensitive channels in older animals. Thus, the subunit switch observed for I_h may serve to uncouple these channels from increasing intracellular cAMP concentrations.

In summary, our results provide a molecular basis for functional changes of I_h during ontogenesis. Additionally, our findings suggest that a subunit switch in the molecular composition of I_h channels takes place that may uncouple I_h from increased intracellular cAMP-mediated signalling.

Acknowledgments

We thank R. Shigemoto for anti-HCN4, and M Hinojosa for editorial assistance. This work was supported by NS35439, NS47993 and DFG SFB505/TP C8.

Abbreviations

4-AP	4-aminopyridine
cAMP	cyclic AMP
HCN channels	hyperpolarization-activated, cyclic nucleotide-gated channels
I_h	h current/hyperpolarization-activated cation current
ISH	*in situ* hybridization
PAGE	polyacrylamide gel electrophoresis
PBS	phosphate-buffered saline
PBS-T	PBS-1% Tween
PIC	Protease Inhibitor Cocktail

SDS	sodium dodecyl sulphate
SSC	saline sodium citrate
TCA	trichloroacetic acid
TEA	tetraethylammoniumchloride
TTX	tetrodotoxin
$V_{1/2}$	midpoint activation voltage
WB	Western blot

References

Agmon A, Wells JE. The role of the hyperpolarization-activated cationic current I(h) in the timing of interictal bursts in the neonatal hippocampus. J. Neurosci 2003;23:3658–3668. [PubMed: 12736337]

Altomare C, Terragni B, Brioschi C, Milanesi R, Pagliuca C, Viscomi C, Moroni A, Baruscotti M, DiFrancesco D. Heteromeric HCN1-HCN4 channels: a comparison with native pacemaker channels from the rabbit sinoatrial node. J. Physiol 2003;549:347–359. [PubMed: 12702747]

Azouz R, Alroy G, Yaari Y. Modulation of endogenous firing patterns by osmolarity in rat hippocampal neurones. J. Physiol 1997;502:175–187. [PubMed: 9234205]

Ben-Ari Y. Excitatory actions of GABA during development: the nature of the nurture. Nat. Rev. Neurosci 2002;3:728–739. [PubMed: 12209121]

Bender RA, Brewster A, Santoro B, Ludwig A, Hofmann F, Biel M, Baram TZ. Differential and age-dependent expression of hyperpolarization- activated, cyclic nucleotide-gated cation channel isoforms 1–4 suggests evolving roles in the developing rat hippocampus. Neuroscience 2001;106:689–698. [PubMed: 11682156]

Bender RA, Galindo R, Mameli M, Gonzalez-Vega R, Valenzuela F, Baram TZ. Synchronized network activity in developing rat hippocampus involves regional hyperpolarization-activated cyclic nucleotide gated (HCN) channel function. Eur. J. Neurosci 2005;22:2669–2674. [PubMed: 16307610]

Bender RA, Soleymani SV, Brewster AL, Nguyen ST, Beck H, Mathern GW, Baram TZ. Enhanced expression of a specific hyperpolarization-activated cyclic nucleotide-gated cation channel (HCN) in surviving dentate gyrus granule cells of human and experimental epileptic hippocampus. J. Neurosci 2003;23:6826–6836. [PubMed: 12890777]

Brewster AL, Bender RA, Chen Y, Dube C, Eghbal-Ahmadi M, Baram TZ. Developmental febrile seizures modulate hippocampal gene expression of hyperpolarization-activated channels in an isoform- and cell-specific manner. J. Neurosci 2002;22:4591–4599. [PubMed: 12040066]

Brewster AL, Bernard JA, Gall CM, Baram TZ. Formation of heteromeric hyperpolarization-activated cyclic nucleotide-gated (HCN) channels in the hippocampus is regulated by developmental seizures. Neurobiol. Dis 2005;19:200–207. [PubMed: 15837575]

Brewster AL, Chen Y, Bender RA, Yeh A, Shigemoto R, Baram TZ. Quantitative analysis and sub-cellular distribution of mRNA and protein expression of the hyperpolarization-activated cyclic nucleotide-gated (HCN) channels throughout development in rat hippocampus. Cerebral Cortex. 2006 in press, epub ahead of print.

Budde T, Caputi L, Kanyshkova T, Staak R, Abrahamczik C, Munsch T, Pape HC. Impaired regulation of thalamic pacemaker channels through an imbalance of subunit expression in absence epilepsy. J. Neurosci 2005;25:9871–9882. [PubMed: 16251434]

Chen S, Wang J, Siegelbaum SA. Properties of hyperpolarizationactivated pacemaker current defined by coassembly of HCN1 and HCN2 subunits and basal modulation by cyclic nucleotide. J. Gen. Physiol 2001;117:491–504. [PubMed: 11331358]

Chen S, Yue C, Yaari Y. A transitional period of Ca^{2+}-dependent spike afterdepolarization and bursting in developing rat CA1 pyramidal cells. J. Physiol 2005;567:79–93. [PubMed: 15919718]

Costa PF, Ribeiro MA, Santos AI. Afterpotential characteristics and firing patterns in maturing rat hippocampal CA1 neurones in in vitro slices. Brain Res. Dev. Brain Res 1991;62:263–272.

Franz O, Liss B, Neu A, Roeper J. Single-cell mRNA expression of HCN1 correlates with a fast gating phenotype of hyperpolarization-activated cyclic nucleotide-gated ion channels (Ih) in central neurons. Eur. J. Neurosci 2000;12:2685–2693. [PubMed: 10971612]

Gravante B, Barbuti A, Milanesi R, Zappi I, Viscomi C, DiFrancesco D. Interaction of the pacemaker channel HCN1 with filamin A. J. Biol. Chem 2004;279:43847–43853. [PubMed: 15292205]

Ishii TM, Takano M, Xie LH, Noma A, Ohmori H. Molecular characterization of the hyperpolarization-activated cation channel in rabbit heart sinoatrial node. J. Biol. Chem 1999;274:12835–12839. [PubMed: 10212270]

Kaupp UB, Seifert R. Molecular diversity of pacemaker ion channels. Annu. Rev. Physiol 2001;63:235–257. [PubMed: 11181956]

Kimura K, Kitano J, Nakajima Y, Nakanishi S. Hyperpolarization- activated, cyclic nucleotide-gated HCN2 cation channel forms a protein assembly with multiple neuronal scaffold proteins in distinct modes of protein-protein interaction. Genes Cells 2004;9:631–640. [PubMed: 15265006]

Lüthi A, McCormick DA. H.-current: properties of a neuronal and network pacemaker. Neuron 1998;21:9–12. [PubMed: 9697847]

Magee JC. Dendritic hyperpolarization-activated currents modify the integrative properties of hippocampal CA1 pyramidal neurons. J. Neurosci 1998;18:7613–7624. [PubMed: 9742133]

Moosmang S, Biel M, Hofmann F, Ludwig A. Differential distribution of four hyperpolarization-activated cation channels in mouse brain. Biol. Chem 1999;380:975–980. [PubMed: 10494850]

Much B, Wahl-Schott C, Zong X, Schneider A, Baumann L, Moosmang S, Ludwig A, Biel M. Role of subunit heteromerization and N-linked glycosylation in the formation of functional hyperpolarizationactivated cyclic nucleotide-gated channels. J. Biol. Chem 2003;278:43781–43786. [PubMed: 12928435]

Notomi T, Shigemoto R. Immunohistochemical localization of I_h channel subunits, HCN1-4, in the rat brain. J. Comp. Neurol 2004;471:241–276. [PubMed: 14991560]

Pape HC. Queer current and pacemaker: the hyperpolarizationactivated cation current in neurons. Annu. Rev. Physiol 1996;58:299–327. [PubMed: 8815797]

Poolos NP, Migliore M, Johnston D. Pharmacological upregulation of h-channels reduces the excitability of pyramidal neuron dendrites. Nat. Neurosci 2002;5:767–774. [PubMed: 12118259]

Proenza C, Angoli D, Agranovich E, Macri V, Accili EA. Pacemaker channels produce an instantaneous current. J. Biol. Chem 2002;277:5101–5109. [PubMed: 11741901]

Qu J, Kryukova Y, Potapova IA, Doronin SV, Larsen M, Krishnamurthy G, Cohen IS, Robinson RB. MiRP1 modulates HCN2 channel expression and gating in cardiac myocytes. J. Biol. Chem 2004;279:43497–43502. [PubMed: 15292247]

Rivera C, Voipio J, Payne JA, Ruusuvuori E, Lahtinen H, Lamsa K, Pirvola U, Saarma M, Kaila K. The K^+ / Cl^- co-transporter KCC2 renders GABA hyperpolarizing during neuronal maturation. Nature 1999;397:251–255. [PubMed: 9930699]

Robinson RB, Siegelbaum SA. Hyperpolarization-activated cation currents: from molecules to physiological function. Annu. Rev. Physiol 2003;65:453–480. [PubMed: 12471170]

Santoro B, Baram TZ. The multiple personalities of h-channels. Trends Neurosci 2003;26:550–554. [PubMed: 14522148]

Santoro B, Chen S, Lüthi A, Pavlidis P, Shumyatsky GP, Tibbs GR, Siegelbaum SA. Molecular and functional heterogeneity of hyperpolarization-activated pacemaker channels in the mouse CNS. J. Neurosci 2000;20:5264–5275. [PubMed: 10884310]

Santoro B, Wainger BJ, Siegelbaum SA. Regulation of HCN channel surface expression by a novel C-terminal protein-protein interaction. J. Neurosci 2004;24:10750–10762. [PubMed: 15564593]

Simeone TA, Sanchez RM, Rho JM. Molecular biology and ontogeny of glutamate receptors in the mammalian central nervous system. J. Child Neurol 2004;19:343–360. [PubMed: 15224708]

Strata F, Atzori M, Molnar M, Ugolini G, Tempia F, Cherubini E. A pacemaker current in dye-coupled hilar interneurons contributes to the generation of giant GABAergic potentials in developing hippocampus. J. Neurosci 1997;17:1435–1446. [PubMed: 9006985]

Surges R, Freiman TM, Feuerstein TJ. K^+-induced changes in the properties of the hyperpolarization-activated cation current I_h in rat CA1 pyramidal cells. Neurosci. Lett 2002;332:136–140. [PubMed: 12384229]

Surges R, Freiman TM, Feuerstein TJ. Input resistance is voltage dependent due to activation of I_h channels in rat CA1 pyramidal cells. J. Neurosci. Res 2004;76:475–480. [PubMed: 15114619]

Ulens C, Tytgat J. Functional heteromerization of HCN1 and HCN2 pacemaker channels. J. Biol. Chem 2001;276:6069–6072. [PubMed: 11133998]

Vasilyev DV, Barish ME. Postnatal development of the hyperpolarization-activated excitatory current I_h in mouse hippocampal pyramidal neurons. J. Neurosci 2002;22:8992–9004. [PubMed: 12388606]

Wainger BJ, DeGennaro M, Santoro B, Siegelbaum SA, Tibbs GR. Molecular mechanism of cAMP modulation of HCN pacemaker channels. Nature 2001;411:805–810. [PubMed: 11459060]

Wang J, Chen S, Nolan MF, Siegelbaum SA. Activity-dependent regulation of HCN pacemaker channels by cyclic AMP: signaling through dynamic allosteric coupling. Neuron 2002;36:451–461. [PubMed: 12408847]

Yu H, Wu J, Potapova I, Wymore RT, Holmes B, Zuckerman J, Pan Z, Wang H, Shi W, Robinson RB, El-Maghrabi MR, Benjamin W, Dixon J, McKinnon D, Cohen IS, Wymore R. MinK-related peptide 1. A beta subunit for the HCN ion channel subunit family enhances expression and speeds activation. Circ. Res 2001;88:E84–E87. [PubMed: 11420311]

Xue T, Marban E, Li RA. Dominant-negative suppression of HCN1- and HCN2-encoded pacemaker currents by an engineered HCN1 construct: insights into structure-function relationships and multimerization. Circ. Res 2002;90:1267–1273. [PubMed: 12089064]

Zhang K, Farooqui SM, O'Donnell JM. Ontogeny of rolipram-sensitive, low-K(m), cyclic AMP-specific phosphodiesterase in rat brain. Brain Res. Dev. Brain Res 1999;112:11–19.

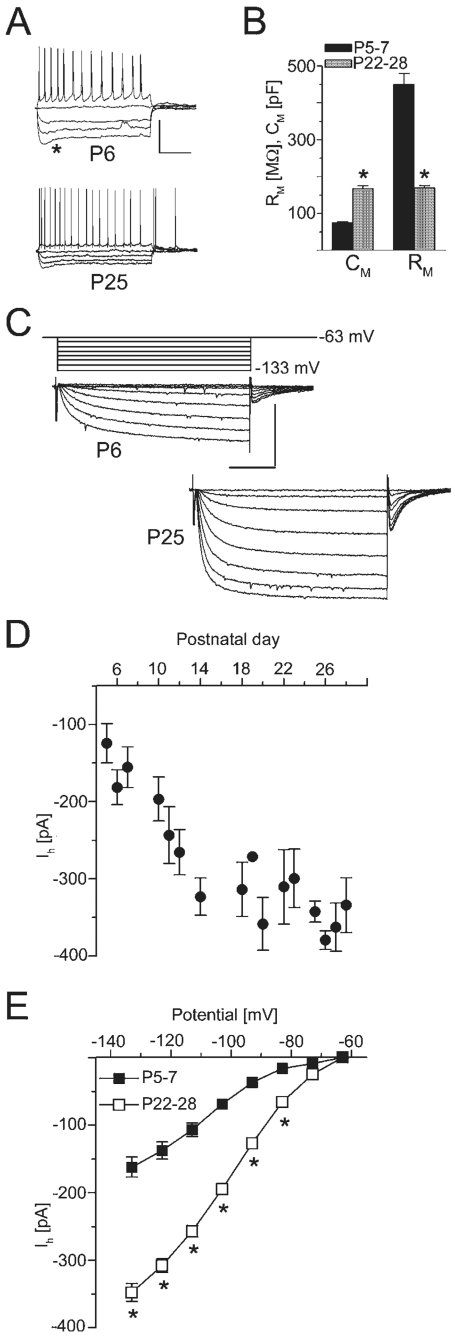

FIG. 1.

Postnatal changes of membrane and I_h properties. (A) Representative examples from P6 (top, RP −69 mV) and P25 (lower traces, RP −74 mV) are shown after current injections (+50 pA to −150 pA). Note the 'voltage sag' attributable to I_h activation (asterisk). Scaling: 50 mV, 400 ms. (B) At P22–28 (n = 33, grey), C_M increased and R_M decreased compared with P5–7 (n = 44, black). (C) In voltage-clamp, hyperpolarization (from −63 mV) evoked slow inward currents in P6 (upper traces) and P25 neurons (lower traces). Scaling: 200 pA, 0.5 s. (D) Plotting averaged amplitudes (−133 mV) vs. age shows increasing I_h amplitude (n = 71, 2–13/point). (E) Plotting averaged I_h amplitudes from P5–7 (filled) and P22–28 (open) vs. command potentials shows increased I_h amplitude with hyperpolarization. P22–28 values

(*n* = 21) were significantly higher than P5–7 (*n* = 20, **P* < 0.001) at most potentials. Error bars = SEM.

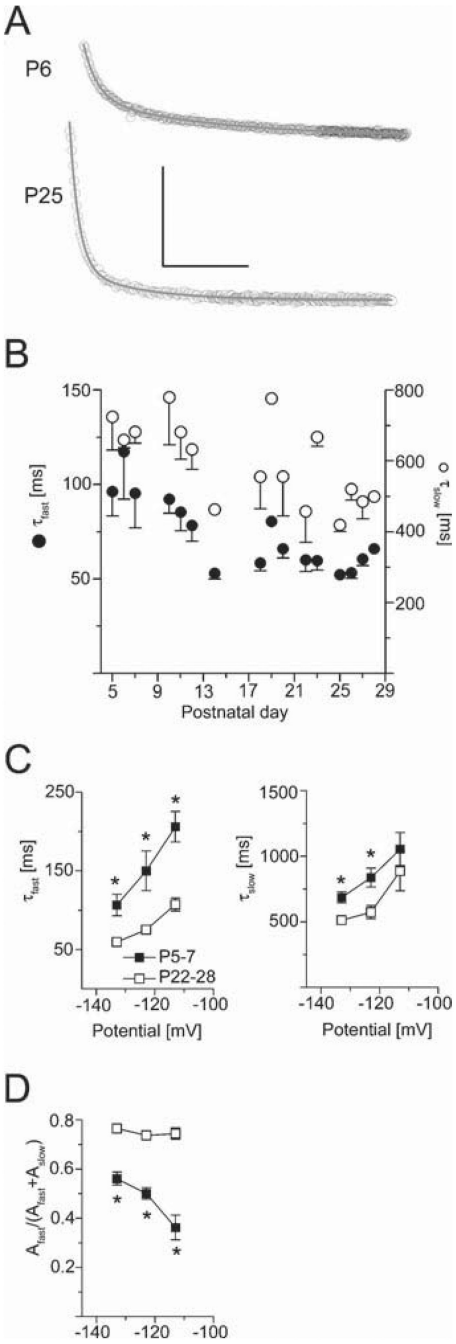

FIG. 2.

I_h activation accelerates during development. (A) Current traces (open symbols) at −133 mV from P6 (upper) and P26 (lower), with superimposed corresponding fits (grey curve). Calibrations 200 pA and 500 ms. (B) τ_{slow} (open circles) and τ_{fast} (filled circles) shortened during development (at −133 mV, n = 71, 2–13 cells/point). (C) Averaged τ_{fast} values from P5–7 (filled squares, n = 20) and P22–28 (open squares, n = 21) were voltage dependent. τ_{fast} (left) shortened with increasing hyperpolarization, being significantly shorter in P22–28 than P5–7 ($P < 0.001$, asterisks). Averaged τ_{slow} values (right) at hyperpolarized potentials were shorter at P22–28 than at P5–7. (D) Average ratios of fast-activating component and

total current amplitudes at P5–7 and P22–28 vs. command potentials. At P22–28 the ratio was significantly larger than at P5–7 (*$P < 0.001$).

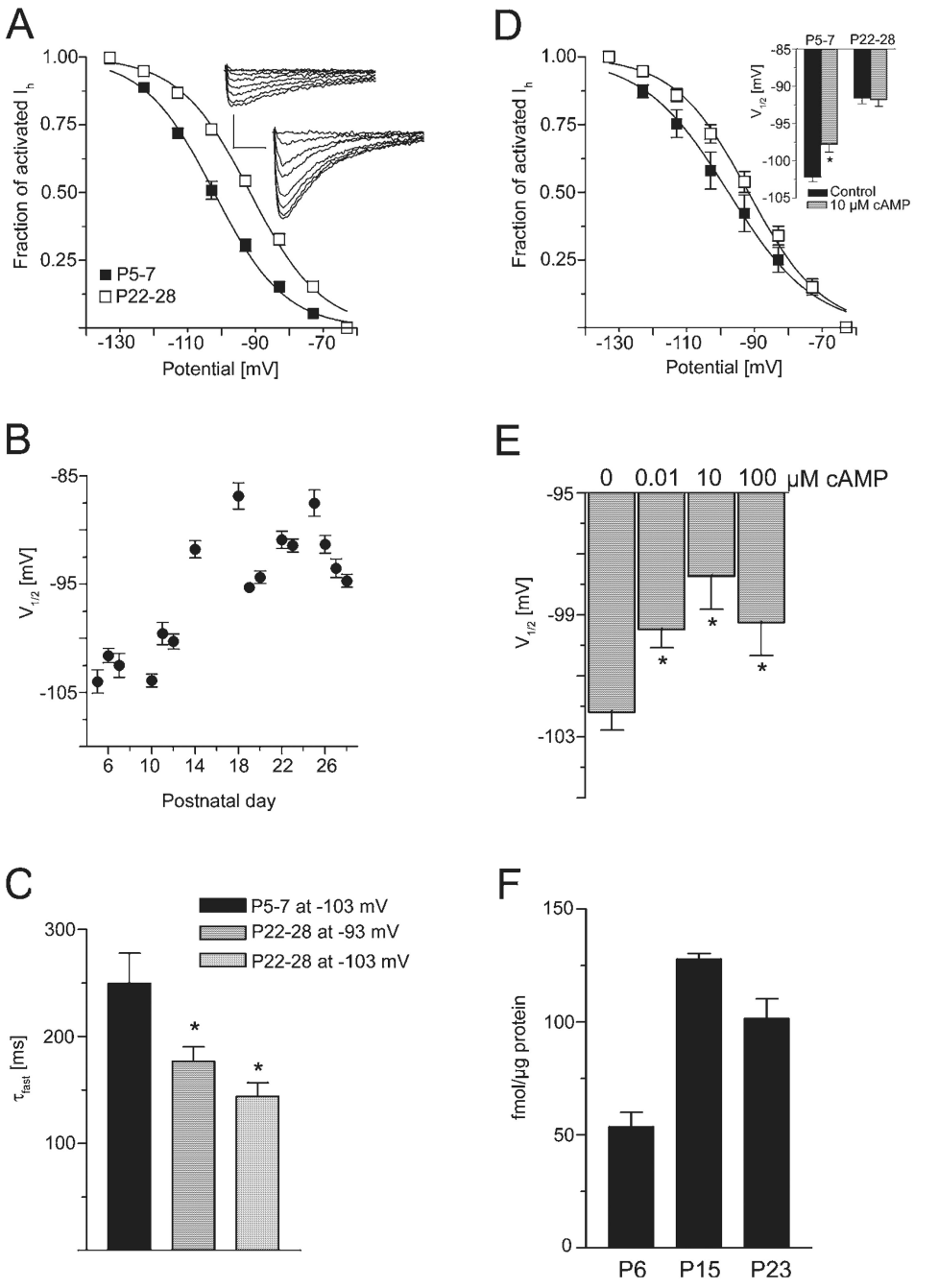

FIG. 3.

Voltage dependence of activation is significantly shifted to depolarized potentials and is less cAMP-sensitive during development. (A) Activation curves revealed that $V_{1/2}$ was shifted in the depolarizing direction at P22–28 (n = 21, open squares) compared with P5–7 (n = 20, filled squares, $P < 0.001$; insets: tail currents at P6 and P25; scaling: 50 pA, 100 ms). (B) Averaged $V_{1/2}$ for each age plotted vs. age, showing a gradual shift of $V_{1/2}$ with age (n = 71, 2–10 cells/point). (C) $\tau_{fast,act}$ at potentials close to $V_{1/2}$: −103 mV at P5–7 (black bars), −103 mV at P22–28 (bright grey bars; dark grey bars at −93 mV). Statistical significance as compared with P5–7 is indicated by asterisks. (D) $V_{1/2}$ was determined in 10 µM cAMP at P5–7 (n = 7, filled squares) and P22–28 (n = 7, open squares). cAMP only affected the

activation curve in immature neurons (inset). (E) $V_{1/2}$ was determined at P5–7 under control conditions (n = 20) and in 0.01 (n = 8), 10 (n = 7) and 100 μM (n = 4) internal cAMP. $V_{1/2}$ shift is already saturated at 10 μM. (F) Hippocampal cAMP levels are age dependent. cAMP was analysed in individual extracts (n = 4/group), under conditions preventing cAMP degradation, by radioimmunoassay. Concentration at P15 was 240% of P6 (*P < 0.001; ANOVA; Bonferroni's *post hoc* test) and did not differ significantly between P15 and P23.

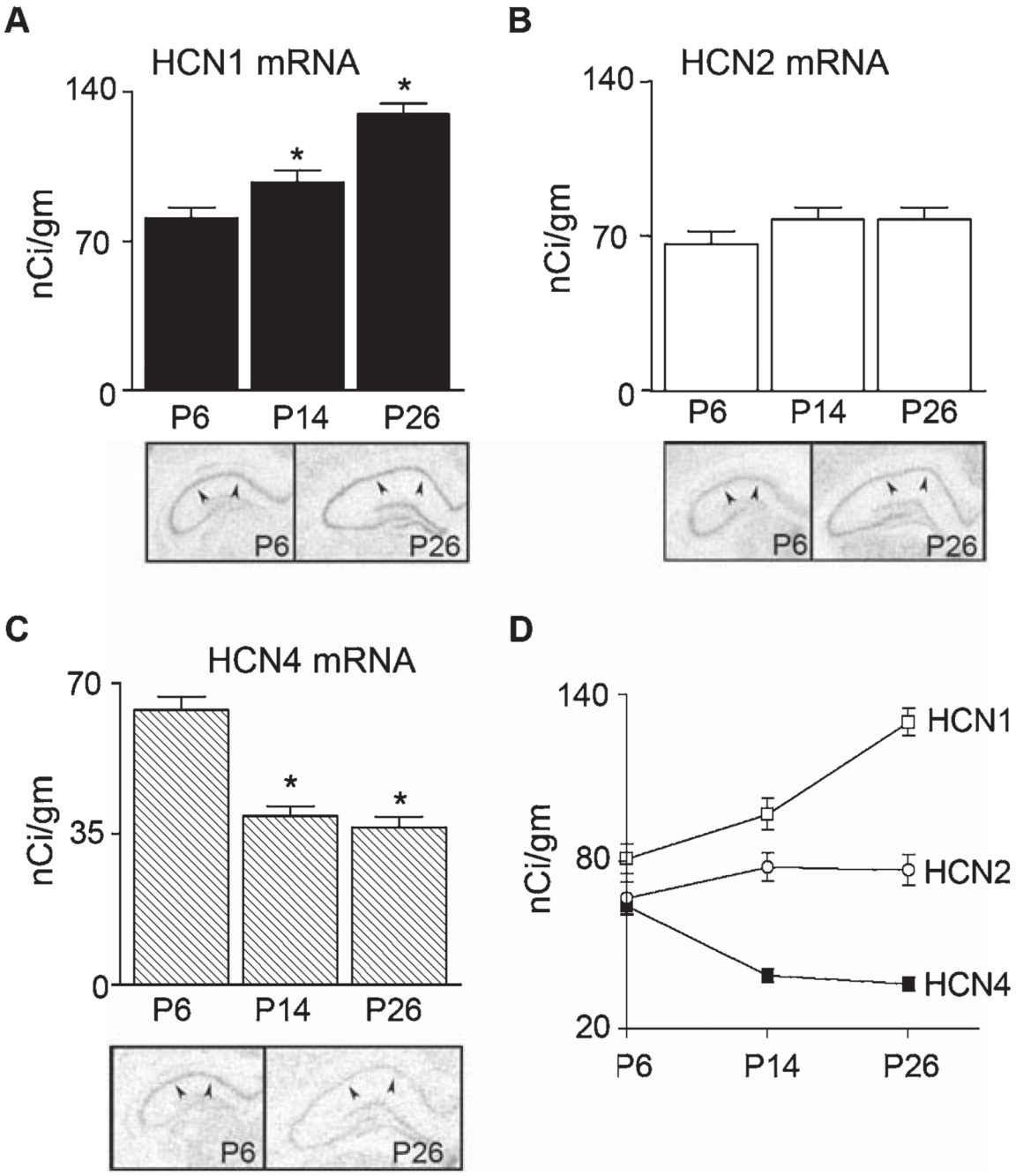

FIG. 4.

Quantitative analysis of age-dependent mRNA expression of hyperpolarization-activated, cyclic nucleotide-gated channels (HCN)1, 2, 4 channel isoforms in CA1 using ISH ($n = 4$/group). The figure shows representative autoradiographs and quantitative analysis for each isoform. (A) HCN1 mRNA levels in CA1 (arrowheads) increased progressively with age ($P < 0.001$). (B) HCN2 mRNA expression tended to increase between P6 and P14, then remained stable, and ANOVA analysis did not show significant changes with age. (C) HCN4 mRNA levels declined as a function of age ($P < 0.0001$). (D) The relative contribution of HCN channel isoform to the total h-channel mRNA pool was age dependent: HCN4 contribution declined from 28.5 to 14%; HCN1 increased from 36 to 50.6%. *Levels

significantly different from P6; †significantly different from P14 (ANOVA, with Bonferroni *post hoc* tests).

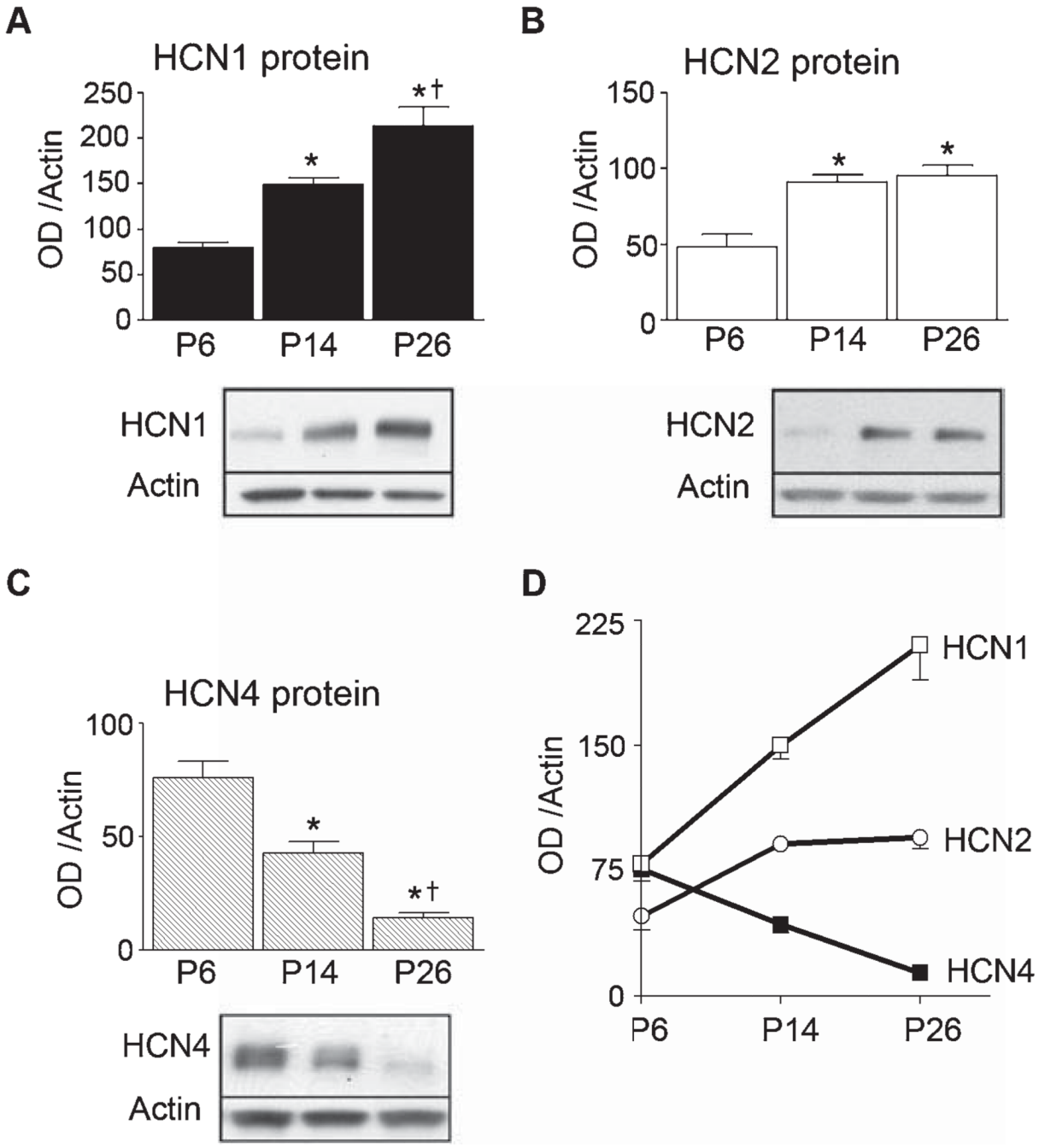

FIG. 5.

Protein levels of the hyperpolarization-activated, cyclic nucleotide-gated channels (HCN)1, 2 and 4 channel isoforms in hippocampal CA1 vary with age. Protein levels were measured in CA1 samples from individual rats, and were expressed in reference to actin levels in the same samples, as shown. (A). HCN1 protein expression, evaluated using Western blots (n = 4–6/age), correlated well with the mRNA, increasing progressively with age ($P < 0.01$) as shown in the gel and the quantitative analysis. (B) HCN2 protein levels, analysed using the Alomone antiserum, increased significantly between P6 and P14, then remained stable. (C) HCN4 protein levels decreased significantly with age. (D) Age-dependent contributions of HCN1, HCN2 and HCN4 channel isoforms to total HCN pool of the HCN channels of CA1

cells. For example, the contribution of the HCN1 isoform is predicted to increase from 39 to 65%, and that of HCN4 to decrease from 37 to 4%. *Protein levels significantly different from P6; †significantly different from P14 ($P < 0.0001$).